

Azide-Modified Poly(diethyl vinylphosphonate) for Straightforward Graft-to Carbon Nanotube Functionalization

Moritz Kränzlein, Thomas M. Pehl, Kerstin Halama, Paula F. Großmann, Tim Kratky, Amelie M. Mühlbach, and Bernhard Rieger*

Rare-earth metal-mediated group-transfer polymerization (REM-GTP) offers distinctive features over common polymerization techniques, such as living character, a broad scope of functional monomers, high activity, excellent control of the polymeric parameters as well as inherent chain-end functionalization. Through the latter, polymers with reactive end-groups become feasible, opening the pathway for further post-polymerization functionalization. In this study, a straightforward graft-to immobilization of the Michael-type polymer poly(diethyl vinylphosphonate) (PDEVP) on multi-walled carbon nanotubes (MWCNT) is reported. Hence, a customized azide initiator is synthesized and studied in the C–H bond activation with various lanthanide-based catalysts and the subsequent polymerization of diethyl vinylphosphonate (DEVP). The successful attachment of the azide end-group is demonstrated via electrospray ionization mass spectrometry (ESI-MS) and the synthesized polymers are subjected to immobilization on multi-walled carbon nanotubes in a graft-to approach. The prepared MWCNT:PDEVP composites are analyzed via thermogravimetric analysis (TGA), elemental analysis (EA), Raman spectroscopy, X-Ray photoelectron spectroscopy (XPS), and transmission electron microscopy (TEM) and the versatility of this approach is shown via the stabilization of MWCNT dispersions in water.

1. Introduction

Poly(diethyl vinylphosphonate) (PDEVP) is an interesting candidate for functionalization of carbon nanotubes, as it is a water-soluble polymer with a tunable lower critical solution temperature (LCST)^[1] and can act as a versatile platform as there are different structural derivatives of the vinylphosphonates reported, which are highly interesting for MWCNT functionalization. An allyl-containing PDEVP derivative has been introduced recently, allowing for sidechain modification of the polymers,^[2] as well as an organic radical polymer obtained via attachment of 2,2,4,4-tetramethylpiperidinyloxy (TEMPO)-units to the vinylphosphonate backbone.^[3] Especially the latter would be highly interesting for the proposed functionalization, as it could offer a covalent attachment of a redox-active polymer to an highly electrical conductive carbon support, thus overcoming organic radical batteries main issues of low active mass and dissolution in the batteries electrolyte.^[4] While generally non-covalent or covalent functionalization

of carbon nanotubes can be applied, the latter offers the advantage of avoiding the use of an additional surfactant which might negatively influence material properties and does not rely on necessary non-covalent polymer-CNT interactions, ultimately allowing high versatility of the polymer used. Furthermore, covalently functionalized carbon nanotubes could be dispersed in a broad variety of solvents due to the solubility of PDEVP.^[5] In order to attach the polymers covalently to the MWCNTs, a defined end-group with specific reactivity is necessary. In the context of carbon nanotube functionalization, azide-based functionalizations for graft-from and graft-to approaches have been investigated thoroughly, as azide moieties can be used either for azide-alkyne click chemistry functionalizations or link to the carbon nanotubes via [2+1] cycloaddition of an in situ formed nitrene.^[6–11] Using these two methods, various different polymers like poly(*N*-isopropylacrylamide),^[12] polycaprolactone,^[13] poly(methyl methacrylate) (copolymers)^[13,14] or polystyrene^[13,15] have successfully been anchored to carbon nanotubes, for further functionalization examples a variety of comprehensive reviews exists in literature.^[10,16] As a versatile functionalization technique for modifying group-transfer polymerization-based

M. Kränzlein, T. M. Pehl, K. Halama, P. F. Großmann, A. M. Mühlbach, B. Rieger

WACKER-Chair of Macromolecular Chemistry
Catalysis Research Center
School of Natural Sciences
Technical University of Munich
Lichtenbergstr. 4, 85748 Garching, Germany
E-mail: rieger@tum.de

T. Kratky
Associate Professorship of Physical Chemistry with Focus on Catalysis
Catalysis Research Center
TUM School of Natural Sciences
Technical University of Munich
Lichtenbergstr. 4, 85748 Garching, Germany

 The ORCID identification number(s) for the author(s) of this article can be found under <https://doi.org/10.1002/mame.202200635>

© 2022 The Authors. Macromolecular Materials and Engineering published by Wiley-VCH GmbH. This is an open access article under the terms of the Creative Commons Attribution License, which permits use, distribution and reproduction in any medium, provided the original work is properly cited.

DOI: 10.1002/mame.202200635

polymers, C–H bond activation of substituted α -methylpyridines has been utilized in literature, successfully introducing a variety of different moieties, including alcohols,^[17,18] amines and thiols,^[18] bipyridines,^[19] di- and tripyridine initiators,^[20,21] or double-bonds^[22] as end-groups. In this approach, an azide-substituted α -methylpyridine is introduced to rare-earth metal-based pre-catalysts like $\text{Cp}_2\text{Ln}(\text{CH}_2\text{TMS})(\text{thf})$ or $[(\text{ONOO})^{\text{tBu}}\text{Ln}(\text{CH}_2\text{TMS})(\text{thf})]$ ($\text{Ln} = \text{Y}, \text{Lu}$) by means of C–H bond activation. These azide-pyridines then act as initiating groups during polymerization initiation and are covalently linked to the polymer chain end via [2+1] cycloaddition of an in situ formed nitrene by nitrogen elimination, acting as functional anchoring groups.^[6–9,18–20,22–24] While this method so far has primarily been used to attach functional moieties like biologically relevant molecules^[18,22] or catalysts^[19] to solvated polymers in a post-polymerization reaction, it could also be utilized to attach end-groups capable of binding to surface for graft-to approaches. PDEVP has successfully been used in a graft-from approach, but so far to the authors knowledge no graft-to methods are known.^[25] Within this manuscript, such a functionalization is introduced in order to covalently couple PDEVP as highly functional REM-GTP-based polymer to multi-walled carbon nanotubes as a proof of principle study.

2. Results and Discussion

2.1. Catalyst Activation and DEVP Polymerization

To be able to introduce the desired azide-moiety to the polymers, a direct approach by C–H bond activation of a functionalized α -methylpyridine is chosen. Starting from 2,6-dimethylpyridine, a chloride is introduced in *para*-position via a literature-known substitution reaction.^[22] The obtained 4-chloro-2,6-dimethylpyridine is reacted with hydrazine-hydrate to the corresponding 4-hydrazineyl-2,6-dimethylpyridine. Without prior isolation, the target molecule 4-azido-2,6-dimethylpyridine (PyN_3) is obtained from a diazotisation with sodium nitrite and 5% hydrochloric acid with a total yield of 20 % after purification by column chromatography.^[26] Formation of the target compound has been confirmed using elemental analysis, gas-chromatography-(GC-MS), ^1H -nuclear magnetic resonance (^1H -NMR), and Fourier-transformed infrared spectroscopy (FT-IR) (see Figures S1 and S2, Supporting Information). To dry the pyridine azide for the subsequent C–H bond activation, it is filtered over activated aluminum oxide and a stock solution in dry benzene- d_6 is prepared (see ESI).

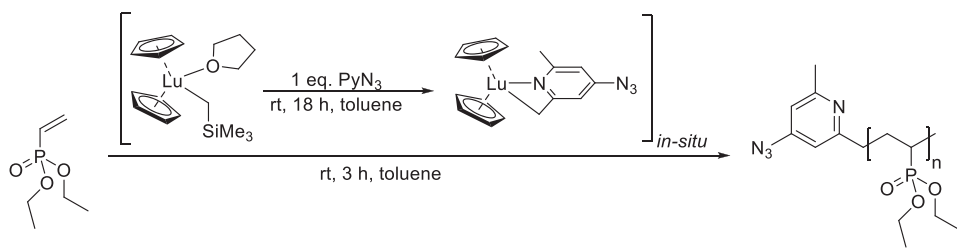
To generate the active polymerization catalyst, an in situ C–H bond activation protocol from literature is used, in which 1.0 equivalents of the functionalized pyridine are reacted with 1.0 equivalents of $\text{Cp}_2\text{Y}(\text{CH}_2\text{TMS})(\text{thf})$ at room temperature.^[18,22] To assess the reactivity, a C–H bond activation kinetic is measured using ^1H -nuclear magnetic resonance spectroscopy at defined time intervals. Surprisingly, the reaction of PyN_3 with $\text{Cp}_2\text{Y}(\text{CH}_2\text{TMS})(\text{thf})$ led to immediate catalyst decomposition as indicated by ^1H -NMR and precipitation of a black solid within seconds. This behavior is attributed to the overall higher reactivity of the azide-pyridine. As the yttrium bis(phenolate) catalyst usually shows a lower reactivity toward C–H bond activation and requires higher activation temperatures of 60 °C,^[23] in

the next step the activation of $[(\text{ONOO})^{\text{tBu}}\text{Y}(\text{CH}_2\text{TMS})(\text{thf})]$ with PyN_3 is tested. Similar to $\text{Cp}_2\text{Y}(\text{CH}_2\text{TMS})(\text{thf})$, upon mixing of the two compounds, the solution immediately turned black, and precipitate formed, indicating catalyst decomposition. This was confirmed using ^1H -NMR spectroscopy. As the last approach, lutetium-based pre-catalysts were tested, as lutetium is known to be less reactive toward C–H bond activation compared to yttrium.^[23] The reaction of $\text{Cp}_2\text{Lu}(\text{CH}_2\text{TMS})(\text{thf})$ with PyN_3 under the same conditions led to the formation of a dark-green solution without precipitation upon mixing of the two reactants overnight at room temperature, indicating successful C–H bond activation. A kinetic investigation of the activation using ^1H -NMR showed complete consumption of PyN_3 within 4 h and formation of tetramethyl silane, revealing the formation of the desired polymerization catalyst (see ESI, Figure S3, Supporting Information). As indicated by the formation of multiple small ^1H -NMR signals in the range of the cyclopentadienyl ligand, some minor side products are formed during the C–H bond activation. These side products were separated by filtration of the catalyst mixture over a syringe filter. To ensure full activation PyN_3 and the lutetium pre-catalyst are reacted for 18 h at room temperature prior to polymerization. Unfortunately, all efforts to isolate the obtained catalyst $\text{Cp}_2\text{Lu}(\text{PyN}_3)(\text{thf})$ to confirm its structure failed as they led to catalyst decomposition. To date, the in situ activation of the azidepyridine remains the only way of obtaining the desired catalyst.

Nevertheless, the in situ generated catalyst is used for the polymerization of diethyl vinylphosphonate (DEVP). The results from the polymerization experiments can be found in **Table 1**.

The polymerizations of DEVP with $\text{Cp}_2\text{Lu}(\text{PyN}_3)(\text{thf})$ at various monomer:catalyst ratios of 25:1, 50:1, 100:1, and 200:1 have been performed in toluene at room temperature. All polymers are characterized regarding their conversion using aliquot- ^{31}P -NMR, molecular structure using $^1\text{H}/^{31}\text{P}$ -NMR (Figures S4 and S5, Supporting Information) and molecular weight and polydispersity using size-exclusion chromatography multi-angle light scattering (SEC-MALS) (Figures S6 and S11, Supporting Information). The catalyst is capable of fully polymerizing the available monomer within 2 h for all monomer:catalyst ratios as indicated by ^{31}P -NMR. All polymers exhibit narrow polydispersity below 1.24, highlighting the controlled polymerization of DEVP by the in situ generated catalyst. Surprisingly, the absolute molecular weights of the polymers $M_{n,\text{abs}}$ are considerably higher than the calculated molecular weights at full initiator efficiency $M_{n,\text{theo}}$, revealing overall low initiator efficiencies of 8.6–14.5%. These initiator efficiencies are about half of the reported literature values for the structural similar lutetium catalyst $\text{Cp}_2\text{Lu}(\text{sym-col})(\text{thf})$ without azide functionalities of 21 %.^[24] These low initiator efficiencies led to the formation of high molecular weight polymers with $M_{n,\text{abs}} > 35 \text{ kg mol}^{-1}$ even at low catalyst:monomer ratios of 25:1. Verification of whether the end-group is attached to the polymer is usually done by ^1H -NMR or diffusion ordered (DOSY)-NMR spectroscopy.^[17,18] However for the herein prepared polymers this approach is not feasible due to the high molecular weight of the polymers and the overall low number of detectable protons of the PyN_3 end-group. Additionally, the intactness of the azide moiety cannot be ensured by means of NMR spectroscopy. Therefore, oligomers of PDEVP initiated by $\text{Cp}_2\text{Lu}(\text{PyN}_3)(\text{thf})$ are prepared by reacting 1.0 equivalents of the catalyst with 5.0

Table 1. Results from DEVP polymerization with in situ generated $\text{Cp}_2\text{Lu}(\text{PyN}_3)$.



Entry	[DEVP]:[Lu] ^a [-]:[-]	$M_{n,theo}$ ^b [kg mol ⁻¹]	$M_{n,abs}$ ^c [kg mol ⁻¹]	\bar{D} [-]	I.E. ^d [%]
1	25:1	4.3	36.7	1.17	11.7
2	50:1	8.4	86.7	1.24	9.7
3	50:1	8.4	58.0	1.19	14.5
4	100:1	16.6	185	1.18	9.0
5	100:1	16.6	192	1.24	8.6
6	200:1	33.0	293	1.14	11.3

^a catalyst-monomer ratio as weighed, 13.5 μmol catalyst in 5 mL toluene, RT, 2 h. ^b theoretical molecular weight via $M_{n,theo} = M_{DEVP} \times X_{DEVP} \times ([DEVP]/[Lu])$. ^c absolute molecular weight $M_{n,abs}$ and polydispersity determined via SEC-MALS (40 °C, THF:H₂O = 1:1 with 9 g L⁻¹ tetra-*n*-butyl ammonium bromide and 272 mg L⁻¹ 2,6-di-*tert*-butyl-4-methylphenol) using $dn/dc = 0.0922 \text{ mL g}^{-1}$ for PDEVP. ^d initiator efficiency as, i.e., = $M_{n,theo}/M_{n,abs} \times 100\%$.

equivalents of monomer and the oligomers are subjected to ESI-MS measurements directly from the reaction mixture (see ESI, Figure S12, Supporting Information). In the electron-spray ionization mass-spectrometry (ESI-MS), two series can be detected, corresponding to PDEVP oligomers initiated by PyN_3 with an intact azide moiety and one series of PDEVP oligomers with the pyridine lacking the azide moiety, presumably due to decomposition in the ESI-MS. While no quantitative functionalization of the polymers with the azide can be verified, still attachment of the azide via C–H bond activation functionalization is generally possible. The prepared polymers from Table 1 are used for further reactions with the multi-walled carbon nanotubes to assess the proposed functionalization pathway.

2.2. Polymer-Carbon Nanotube Coupling and Characterization

To covalently link the prepared polymers to the multi-walled carbon nanotubes, a [2+1] cycloaddition between the π -electrons of the carbon nanotubes and an in situ formed nitrene by thermally induced nitrogen extrusion of the polymers azide moiety is performed (see ESI).^[6–9] Different weight-percent ratios of MWCNT:PDEVP of 1:1, 1:2, and 1:5 of PDEVP with a molecular weight of 192 kg mol⁻¹ (PDEVP₁₀₀, Table 1, entry 5) are tested as well as additional 1:5 ratios with different polymer chain lengths of 58.0 kg mol⁻¹ (PDEVP₅₀, Table 1, entry 3) and 293 kg mol⁻¹ (PDEVP₂₀₀, Table 1, entry 6). To assess the loading of the nanotubes with the polymer, elemental analysis of the C, H, N, and P content of all prepared compounds is measured, and the loading is calculated based on the phosphorus percentage found (Table 2).

As an additional method of quantification, the prepared composites are subject to thermogravimetric analysis under an argon atmosphere, the corresponding graphs are shown in Figure 1.

Pure MWCNTs do not show any decomposition up to 850 °C under argon, while pure PDEVP starts to decompose by loss of

its ethyl side chains at 260 °C as indicated by a weight loss of 38 wt.%. Starting at about 450 °C, a second decomposition onset can be detected, attributed to thermal fragmentation of the backbone, followed by a less defined decomposition step at about 800 °C, leaving a carbon residue of 18%.^[27] Using the first decomposition step of 38 wt.% for pure PDEVP, the relative content of PDEVP on the MWCNTs can be calculated by determining the weight percent difference before and after the first decomposition step and dividing it by 38 wt.%. The loadings determined from elemental analysis and from TGA are compared to each other, the corresponding results are listed in Table 3.

Comparison of the loadings determined from EA and TGA shows quite good agreement with deviations of only about 5 wt.%, which are attributed to measurement uncertainties. Overall, the compounds with the lowest initial MWCNT:PDEVP ratio of PDEVP₁₀₀ also show the lowest loading of ≈ 10 wt.% of polymer content. The two experiments with higher MWCNT:PDEVP ratio (1:2 and 1:5) of PDEVP₁₀₀ achieve about the same degree of functionalization with 21–22 wt.% of polymer. This might be due to steric blocking/coverage of the MWCNT surface by the polymers, impeding azide end-groups from reacting with the MWCNT surface, thus making a higher degree of functionalization impossible. When using shorter-chain PDEVP₅₀ in a 1:5 ratio, about the same wt.% of polymer can be detected, corresponding to a higher surface density of functionalized polymer on the carbon nanotubes. This might be due to an overall much shorter chain length of PDEVP₅₀ compared to PDEVP₁₀₀ and therefore less sterical hindrance during the graft-to functionalization. For the longest PDEVP₂₀₀, 42 wt.% of polymer loading were determined due to the overall higher molecular weight of the polymer with a similar degree of functionalization as for the MWCNT:PDEVP 1:2 and 1:5 loadings.

Additionally, the functionalization of the carbon nanotubes is investigated using Raman spectroscopy, XPS, and TEM. To access whether MWCNTs have successfully been functionalized, Raman spectra of pure MWCNTs and of MWCNT:PDEVP₁₀₀ = 1:2

Table 2. Elemental analysis results of the MWCNT:PDEVP composites prepared.

Entry	Compound	MWCNT:PDEVP [wt.%]:[wt.%]		C [%]	H [%]	N [%]	P [%]	Loading ^a [wt.%]:[wt.%]
1	pure MWCNTs	1:0	Calculated ^b	100	0.00	0.00	0.00	-
			Found ^c	95.77	0.04	0.00	0.00	-
2	pure PDEVP	0:1	Calculated ^b	43.90	7.98	0.00	18.87	-
			Found ^c	41.15	8.05	0.12	16.85	-
3	MWCNT:PDEVP ₁₀₀	1:1	Calculated ^b	69.00	3.99	0.00	9.43	50:50
			Found ^c	87.65	1.23	0.20	2.58	85:15
4	MWCNT:PDEVP ₁₀₀	1:2	Calculated ^b	61.47	5.19	0.00	12.27	35:65
			Found ^c	80.70	1.90	0.20	4.84	76:24
5	MWCNT:PDEVP ₁₀₀	1:5	Calculated ^b	53.94	6.38	0.00	15.10	20:80
			Found ^c	80.06	1.99	0.00	4.80	75:25
6	MWCNT:PDEVP ₅₀	1:5	Calculated	53.94	6.38	0.00	15.10	20:80
			Found	81.71	1.66	0.23	4.15	79:21
7	MWCNT:PDEVP ₂₀₀	1:5	Calculated	53.94	6.38	0.00	15.10	20:80
			Found	70.81	3.40	0.15	7.33	57:43

^a loading determined from the wt.% phosphorus found in elemental analysis. ^b expected elemental composition of C, H, N, and P based on the wt.:%wt.:% ratios used in the experiments. ^c determined C, H, N, P content from single determination elemental analysis.

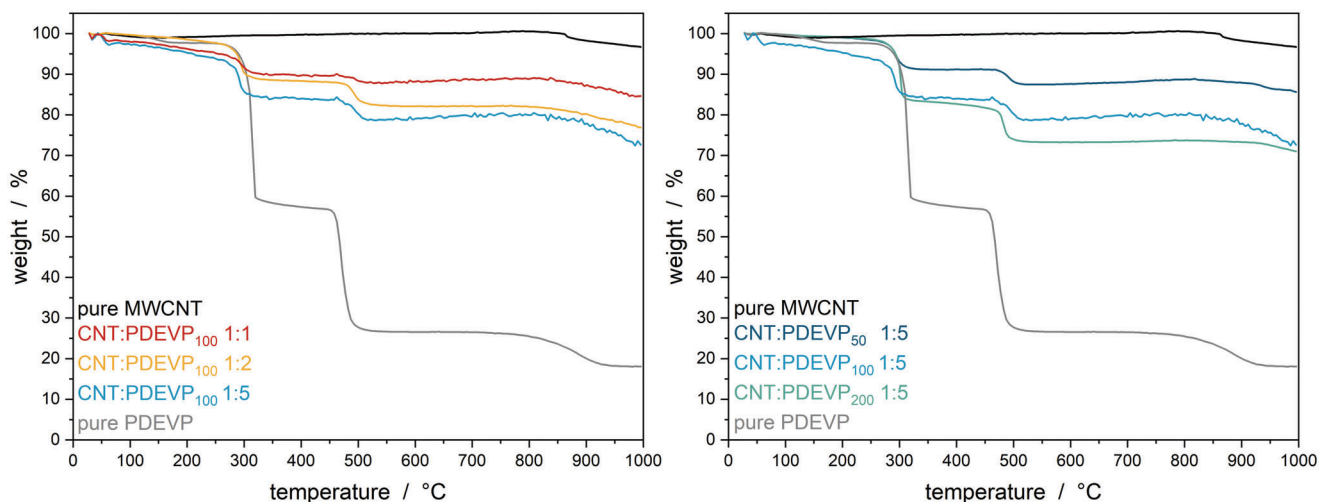


Figure 1. TGA measurements of PDEVP-MWCNT composite materials with varying polymer chain lengths at constant MWCNT:PDEVP ratio (left) and with varying MWCNT:PDEVP functionalization ratios of the same polymer (right).

Table 3. Comparison of MWCNT:PDEVP loading determined via elemental analysis and thermogravimetric analysis.

Entry	Compound	MWCNT:PDEVP [wt.%]:[wt.%]	Loading from EA [wt.%]:[wt.%]	Loading from TGA [wt.%]:[wt.%]
1	MWCNT:PDEVP ₁₀₀	1:1	85:15	90:10
2	MWCNT:PDEVP ₁₀₀	1:2	76:24	79:21
3	MWCNT:PDEVP ₁₀₀	1:5	75:25	78:22
4	MWCNT:PDEVP ₅₀	1:5	79:21	78:22
5	MWCNT:PDEVP ₂₀₀	1:5	57:43	58:42

(Table 2, entry 4) in the range of 1000–1800 cm^{-1} are measured (Figure S13, Supporting Information). In the Raman spectra, the band at around 1326 cm^{-1} can be assigned to the G band of the sp^2 -bonded carbon atoms within the CNT surface layers, while the band between 1570–1610 cm^{-1} can be assigned to the D band of sp^3 -hybridized carbon atoms of defects of the carbon nanotubes.^[11,13,28] When comparing the D band of pristine MWCNTs with the MWCNT:PDEVP₁₀₀ = 1:2 D band, a slight shift of the band can be observed. While the pure MWCNTs exhibit a single D band with a slight shoulder at higher Raman shifts, for the hybrid material the emergence of an additional band can be observed. This is attributed to a covalent functionalization of the MWCNTs with the polymer via [2+1] cycloaddition, however, this has to be considered with care as the overall amount of new defects due to covalent bonding is

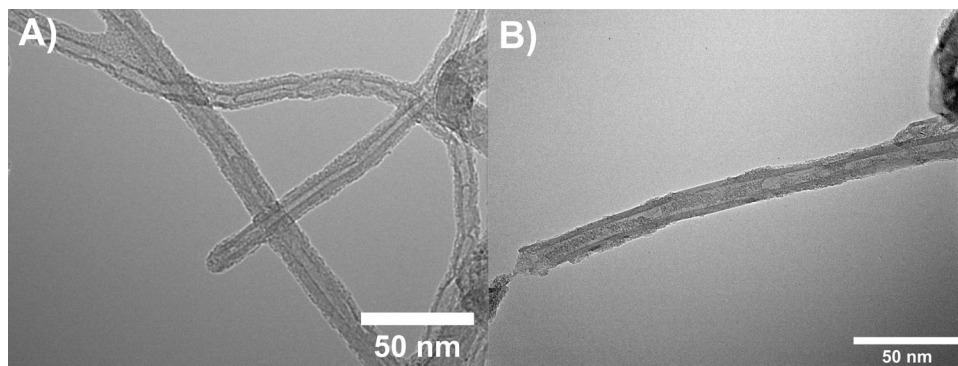


Figure 2. A). TEM images of pristine MWCNTs before functionalization and B) after functionalization with PDEVP₂₀₀ (Table 2, entry 7).

very low compared to the overall surface of the MWCNTs.^[13] XPS analysis of pristine carbon nanotubes, pure PDEVP, and the MWCNT:PDEVP₁₀₀ = 1:5 compound material reveals the formation of a hybrid material (Figure S14, Supporting Information), while the attachment point via the nitrogen itself could not be found due to the small quantity of attachment units compared to the overall mass of the MWCNTs and the polymer. Quantification of the corresponding C 1s components gives an MWCNT:PDEVP₁₀₀ ratio of 40:60 ([at% C]:[at% C]) which is substantially lower compared to a ratio of 87:13 ([at% C]:[at% C]) as observed by elemental analysis. The higher fraction of polymer found in XPS evidences a structure of the composite material in which the polymer covers the MWCNT surface leading to an attenuation of the C 1s signal intensity of the MWCNT components. In the TEM pictures, the pristine MWCNT (Figure 2A) exhibits a typical homogeneous structure of multiwalled carbon nanotubes featuring a smooth surface with a diameter of 20 nm, for the MWCNT functionalized with PDEVP₂₀₀ (Table 2, entry 7) heterogeneous surface species can be observed (Figure 2B). The higher absorption of the TEM electron beam can be induced by higher adsorption of the phosphorous-containing PDEVP. In addition, TEM allows for a rough estimation of the surface species size, resulting in a diameter of 2 nm and a length of 30 nm, which is in good agreement with the hydrodynamic radius of PDEVP₂₀₀ derived via SEC-MALS. Thus, the authors conclude that the attached surface species is the grafted poly(diethyl vinylphosphonate). The overall high coverage of the MWCNT's surface with the polymer species is in good agreement with the previously observed limit for further polymer immobilization due to steric blocking of the MWCNT surface by, e.g., wrapping.^[29]

2.3. Suspension Experiments

In the final step, the functionalized carbon nanotubes are suspended in water to assess the capability of the water-soluble PDEVP to stabilize the nanotubes against coagulation. Suspensions of 0.05 mg mL⁻¹ of the MWCNT:PDEVP compound materials in Millipore water are prepared and pictures are taken immediately after suspension, 5 min, 3 h, and 24 h (Figure 3). The composites from the 1:5 MWCNT:PDEVP loadings at different chain lengths (A–C) and the composites from the 1:2 and the 1:1 loading with PDEVP₁₀₀ (D, E) are compared to the pure MWC-

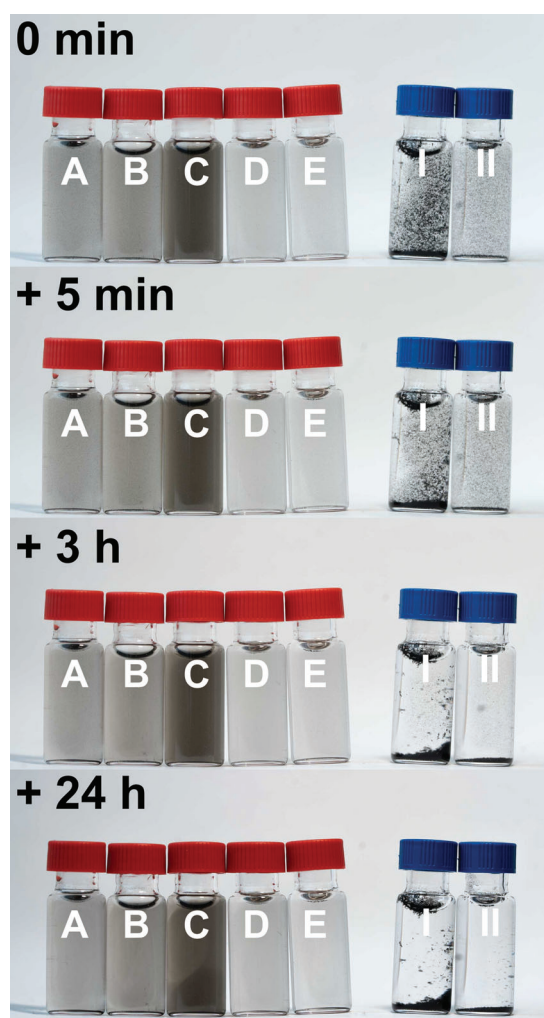


Figure 3. A) MWCNT:PDEVP₂₀₀ = 1:5 (Table 2, entry 7); B) MWCNT:PDEVP₁₀₀ = 1:5 (Table 2, entry 5); C) MWCNT:PDEVP₅₀ = 1:5 (Table 2, entry 6); D) MWCNT:PDEVP₁₀₀ = 1:2 (Table 2, entry 4); E) MWCNT:PDEVP₁₀₀ = 1:1 (Table 2, entry 3), I pure MWCNTs without polymer functionalization; II MWCNTs after functionalization with a non-azide functionalized PDEVP as control experiment.

NTs in water (I) and a mixture of carbon nanotubes with non-functionalized PDEVp ($M_{n,abs} = 121 \text{ kg mol}^{-1}$, $\bar{D} = 1.09$) of 1:5 (II) using the same functionalization protocol. Each of the control experiments I and II show immediate coagulation of the carbon nanotubes, forming unstable suspensions. The compounds from lower MWCNT:PDEVp ratios D and E show a lower stabilizing effect, while the compounds from the 1:5 loadings A–C show a good stabilization of the carbon nanotubes in water. This behavior is attributed to an overall higher degree of functionalization from the experiments where more polymer is used for the surface modification. Additionally, we tried triggering the LCST effect of the surface bound PDEVp by heating the samples to 60 °C. Unfortunately, no defined precipitation of the polymer-MWCNT composites could be observed. Overall, the attached PDEVp chains are capable of stabilizing the carbon nanotubes against coagulation, forming stable suspensions, yet the LCST effect of PDEVp is not retained.

3. Conclusion

By means of group-transfer polymerization of DEVp with an in situ generated C–H bond activation-based catalyst from $\text{Cp}_2\text{Lu}(\text{CH}_2\text{TMS})(\text{thf})$ and an azide-substituted pyridine, poly(diethyl vinylphosphonate) was successfully functionalized with an azide polymer end-group. By using a thermally induced nitrene [2+1] cycloaddition, the PDEVps prepared were covalently linked to MWCNTs via the azide moiety in a graft-to approach. Different polymer chain lengths and polymer to carbon nanotubes have been tested in the functionalization and the loaded compounds were characterized using elemental analysis, thermogravimetric analysis, transmission electron microscopy, raman spectroscopy, and X-ray photoelectron spectroscopy. The polymer on the surface on the carbon nanotube is capable of stabilizing suspensions of MWCNTs in water against coagulation. The herein-presented pathway toward MWCNT functionalization with GTP-based polymers could provide a synthetic tool toward more advanced materials like organic radical polymers immobilized on carbon nanotubes to overcome one of the limiting components of organic radical batteries. Further, the azide functionality itself is an immensely useful building block in organic chemistry to further functionalize organic (macro)molecules via copper-mediated click chemistry, thus opening a feasible pathway for further research.

Supporting Information

Supporting Information is available from the Wiley Online Library or from the author.

Acknowledgements

The authors want to thank Maximilian Stierle for his help with preparing the pyridine azide. Funding Sources: M.K. is grateful for the Ph.D. scholarship from the Studienstiftung des Deutschen Volkes.

Open access funding enabled and organized by Projekt DEAL.

Conflict of Interest

The authors declare no conflict of interest.

Author Contributions

M.K., T.M.P., and K.H., contributed equally to this work. The manuscript was written through the contributions of all authors. All authors have given approval for the final version of the manuscript.

Data Availability Statement

The data that support the findings of this study are available from the corresponding author upon reasonable request.

Keywords

biscyclopentadienyl lutetium catalysts, carbon nanotubes, polymer-composites, polymer-functionalization, polymerization catalysis, rare-earth metal-mediated group-transfer polymerization

Received: November 3, 2022

Revised: December 9, 2022

Published online: December 22, 2022

- [1] N. Zhang, S. Salzinger, B. Rieger, *Macromolecules*. **2012**, *45*, 9751.
- [2] K. Halama, A. Schaffer, B. Rieger, *RSC Adv.* **2021**, *11*, 38555.
- [3] T. M. Pehl, F. Adams, M. Kränzlein, B. Rieger, *Macromolecules*. **2021**, *54*, 4089
- [4] C. Friebe, U. S. Schubert, *Top. Curr. Chem.* **2017**, *375*, 19.
- [5] a) B. Vigolo, V. Mamane, F. Valsaque, T. N. H. a Le, J. Thabit, J. Ghanbaja, L. Aranda, Y. Fort, E. Mcrae, *Carbon*. **2009**, *47*, 411.; b) P. Bilalis, D. Katsigiannopoulos, A. Avgeropoulos, G. Sakellariou, *RSC Adv.* **2014**, *4*, 2911;
- [6] M. Holzinger, J. Abraham, P. Whelan, R. Graupner, L. Ley, F. Henrich, M. Kappes, A. Hirsch, *J. Am. Chem. Soc.* **2003**, *125*, 8566.
- [7] J. Park, M. Yan, *Acc. Chem. Res.* **2013**, *46*, 181.
- [8] S. J. Pastine, D. Okawa, B. Kessler, M. Rolandi, M. Llorente, A. Zettl, J. M. J. Fréchet, *J. Am. Chem. Soc.* **2008**, *130*, 4238.
- [9] A. Setaro, M. Adeli, M. Glaeske, D. Przyrembel, T. Bisswanger, G. Gordeev, F. Maschietto, A. Faghani, B. Paulus, M. Weinelt, R. Arenal, R. Haag, S. Reich, *Nat. Commun.* **2017**, *8*, 14281.
- [10] J. Han, C. Gao, *N.-M. Lett.* **2010**, *2*, 213.
- [11] I. Kumar, S. Rana, C. V. Rode, J. W. Cho, *J. Nanosci. Nanotechnol.* **2008**, *8*, 3351.
- [12] X. Su, Y. a Shuai, Z. Guo, Y. Feng, *Molecules* **2013**, *18*, 4599.
- [13] C. Gao, H. He, L. i Zhou, X. Zheng, Y. u Zhang, *Chem. Mater.* **2009**, *21*, 360.
- [14] G. Li, H. u Wang, H. Zheng, R. Bai, *Langmuir* **2010**, *26*, 7529.
- [15] H. Li, F. Cheng, A. M. Duft, A. Adronov, *J. Am. Chem. Soc.* **2005**, *127*, 14518.
- [16] a) N. G. Sahoo, S. Rana, J. W. Cho, L. Li, S. H. Chan, *Prog. Polym. Sci.* **2010**, *35*, 837; b) A. M. Díez-Pascual, *Macromol.* **2021**, *1*, 64; c) Z. Abousalman-Rezvani, P. Eskandari, H. Roghani-Mamaqani, M. Salami-Kalajahi, *Adv. Colloid. Interface. Sci.* **2020**, *278*, 102126; d) S. Campidelli, *COC.* **2011**, *15*, 1151;
- [17] T. M. Pehl, M. Kränzlein, F. Adams, A. Schaffer, B. Rieger, *Catalysts* **2020**, *10*, 448.
- [18] A. Schaffer, M. Kränzlein, B. Rieger, *Macromolecules*. **2020**, *53*, 4345.
- [19] F. Adams, M. Pschenitzka, B. Rieger, *ChemCatChem.* **2018**, *10*, 4309.
- [20] P. Pahl, C. Schwarzenböck, F. A. D. Herz, B. S. Soller, C. Jandl, B. Rieger, *Macromolecules*. **2017**, *50*, 6569.
- [21] a) A. Saurwein, A. Schaffer, C. Wieser, B. Rieger, *RSC Adv.* **2021**, *11*, 1586; b) P. T. Altenbuchner, P. D. L. Werz, P. Schöppner, F. Adams,

- A. Kronast, C. Schwarzenböck, A. Pöthig, C. Jandl, M. Haslbeck, B. Rieger, *Chemistry* **2016**, 22, 14576;
- [22] C. Schwarzenböck, A. Schaffer, P. Pahl, P. J. Nelson, R. Huss, B. Rieger, *Polym. Chem.* **2018**, 9, 284.
- [23] F. Adams, M. R. Machat, P. T. Altenbuchner, J. Ehrmaier, A. Pöthig, T. N. V. Karsili, B. Rieger, *Inorg. Chem.* **2017**, 56, 9754.
- [24] B. S. Soller, S. Salzinger, C. Jandl, A. Pöthig, B. Rieger, *Organometallics* **2014**, 34, 2703.
- [25] N. Zhang, S. Salzinger, B. S. Soller, B. Rieger, *J. Am. Chem. Soc.* **2013**, 135, 8810.
- [26] H. Sawanishi, K. Tajima, T. Tsuchiya, *Chem. Pharm. Bull.* **1987**, 35, 3175.
- [27] D. Lanzinger, S. Salzinger, B. S. Soller, B. Rieger, *Ind. Eng. Chem. Res.* **2015**, 54, 1703.
- [28] M. S. Dresselhaus, G. Dresselhaus, R. Saito, A. Jorio, *Phys. Rep.* **2005**, 409, 47.
- [29] M. Raimondo, C. Naddeo, L. Vertuccio, L. Bonnaud, P. Dubois, W. H. Binder, A. Sorrentino, L. Guadagno, *Nanotechnology* **2020**, 31, 225708.